



Geochemistry

Duration and synchronicity of the largest negative carbon isotope excursion on Earth: The Shuram/Wonoka anomaly

Durée et synchronisme de la plus grande excursion négative terrestre des isotopes du carbone : l'anomalie Shuram/Wonoka

Erwan Le Guerroué*

Geosciences-Rennes (UMR6118 du CNRS), 263, avenue du General-Leclerc, CS 74205, 35042 Rennes cedex, France

ARTICLE INFO

Article history:

Received 26 September 2008

Accepted after revision 7 December 2009

Available online 12 March 2010

Presented by Vincent Courtillot

Keywords:

Strontium isotopes
Carbon isotope
Neoproterozoic
Ediacaran
Shuram
Wonoka

Mots clés :

Isotopes du strontium
Isotope du carbone
Néoprotérozoïque
Édiacaran
Shuram
Wonoka

ABSTRACT

Carbonate $\delta^{13}\text{C}$ values provide a useful monitor of changes in the global carbon cycle because they can record the burial ratio of organic to carbonate carbon. The most pronounced isotope excursions in the geologic record occur during the Neoproterozoic and have assumed a central role in the interpretation of biogeochemical events preceding the Ediacaran and Cambrian radiations. The most profound negative carbon isotope excursion is best recorded in the Ediacaran-aged Shuram Formation of Oman and has potential equivalents worldwide including the Wonoka Formation of South Australia and other sections in China, India, Siberia, Canada, Scandinavia and Brazil. All these excursions are less well understood than those in the Phanerozoic because of their unusual magnitude, long duration (> 1 Ma) and the difficulty in correlating Neoproterozoic basins to confirm independently that they do indeed record global change in the mixed ocean reservoir. Alternatively, these $\delta^{13}\text{C}$ anomalies could reflect diachronous diagenetic processes. Currently none of these excursion are firmly time constrained and critical to their interpretation is a coherent reproducibility and synchronicity at the global ocean scale. Here we use available strontium isotope record as an independent chronometer to test the timing and synchronicity of the Shuram $\delta^{13}\text{C}$ and its potential equivalents. The use of the $^{86}\text{Sr}/^{87}\text{Sr}$ ratio allows the reconstruction of a coherent, global $\delta^{13}\text{C}$ record calibrated independently against time. The calibrated $\delta^{13}\text{C}$ curve indicates that the Shuram negative anomaly spans several tens of millions of years and reaches values below -10‰ . This carbon isotopic anomaly therefore represents a meaningful oceanographic event that fundamentally challenges our understanding of the carbon cycle as defined in the Phanerozoic.

© 2010 Académie des sciences. Published by Elsevier Masson SAS. All rights reserved.

R É S U M É

Les valeurs du $\delta^{13}\text{C}$ mesurées dans les carbonates marins permettent de suivre les variations du cycle du carbone à l'échelle mondiale, en témoignant de l'enfouissement du carbone carbonaté par rapport au carbone organique. Dans l'enregistrement géologique, les excursions isotopiques les plus prononcées sont observées au Néoprotérozoïque. Ces excursions ont joué un rôle prépondérant dans l'interprétation des événements biogéochimiques et coïncident avec les radiations édiacariennes et cambriennes. La plus

* Present address: Beicip-Franlab, 232, avenue Napoléon-Bonaparte, PO Box 213, 92502 Rueil-Malmaison, France.

E-mail address: erwan.le_guerroue@alumni.ethz.ch.

prononcée des excursions négatives du $\delta^{13}\text{C}$ est enregistrée à l'Édiacarien dans la Formation de Shuram en Oman. Cette excursion a des équivalents potentiels sur différents fragments continentaux, tels que la Formation de Wonoka en Australie du Sud. Ces excursions négatives demeurent plus compliquées à interpréter que leur équivalent Phanérozoïque en raison de leur amplitude inhabituelle, de leur longue durée (> 1 Ma) et de la difficulté à corréler les bassins néoprotozoïques de façon indépendante. Ces corrélations sont pourtant indispensables pour confirmer un changement global du $\delta^{13}\text{C}$ du réservoir océanique mixte global. Au contraire, ces excursions pourraient refléter des processus diagénétiques diachroniques. Vérifier la cohérence, la reproductibilité et le synchronisme à l'échelle globale de ces excursions constitue un test critique de leur véracité. Ici, nous utilisons l'enregistrement isotopique du strontium en tant que chronomètre indépendant, pour tester le synchronisme du signal du $\delta^{13}\text{C}$ de la Formation de Shuram et de ses équivalents potentiels. L'utilisation du rapport $^{86}\text{Sr}/^{87}\text{Sr}$ permet de composer une variation globale, cohérente et contrainte dans le temps. Les résultats montrent que l'anomalie négative du $\delta^{13}\text{C}$ s'étend sur plusieurs dizaines de millions d'années, atteignant des valeurs inférieures à -10% . Cette anomalie composite du $\delta^{13}\text{C}$ représente donc un événement océanographique primaire qui remet profondément en question la compréhension du cycle du carbone telle qu'elle est définie dans le Phanérozoïque.

© 2010 Académie des sciences. Publié par Elsevier Masson SAS. Tous droits réservés.

1. Introduction

There is widespread interest in the Neoproterozoic period of the Earth's history (1000 to 542 Ma) because of seemingly unprecedented environmental fluctuations. Many believe these environmental perturbations to be responsible for the changing conditions in the biosphere that facilitated the radiation of metazoan life (animals) towards the end of the Neoproterozoic (Fike et al., 2006; Kennedy et al., 2006; Knoll and Carroll, 1999; Peltier et al., 2007) (Fig. 1). The carbon isotopic record of ancient ocean water preserved in marine carbonates serves as an important means to recognize changes in the exogenic cycle coincident with these evolutionary events (Knoll et al., 1986; Magaritz, 1991; Peltier et al., 2007; Schidlowski and Aharon, 1992). The Neoproterozoic $\delta^{13}\text{C}$ record shows several unprecedented fluctuations (Halverson et al., 2005; Le Guerroué et al., 2006c; Shields and Veizer, 2002) (Fig. 1) with implications especially interesting in the Ediacaran interval (635–542 Ma), during which atmospheric oxygen concentrations were likely to have been particularly dynamic (Bartley and Kah, 2004; Rothman et al., 2003) (Fig. 1), ultimately stabilizing closer to modern levels (Canfield and Teske, 1996; Kah et al., 2004). A step to higher oxygen concentration is widely believed to be a necessary condition for multicellularity and metazoan evolution (Anbar and Knoll, 2002; Kennedy et al., 2006; Knoll and Walter, 1992) and to be important in determining the timing of the first animals in the fossil record.

The most negative $\delta^{13}\text{C}$ excursion in the Neoproterozoic (e.g. the "Shuram/Wonoka Excursion" (Le Guerroué et al., 2006c); Fig. 1) fundamentally challenges the standard understanding of isotopic mass balance as established in the modern ocean (Broecker and Peng, 1982). The long time scale required by the stratigraphic complexity of the excursion, largely longer than the residence time of carbon in the ocean is $\approx 10^5$ y, implies that these strongly negative isotopic values (below -10%) record a sustainable steady state condition in the global ocean. This contrasts sharply

with the rare, short-lived, excursions of only $\sim 4\%$ accepted in the Phanerozoic (Hayes et al., 1999; Veizer et al., 1999; Zachos et al., 2001) (Fig. 1). These Phanerozoic excursions have been used as evidence only for transient (short term) global ecosystem disruptions while large negative values recorded in Phanerozoic carbonates, have been interpreted as diagenetic alteration (see good example in Swart and Eberli, 2005, and being the product of processes not constrained by the global isotopic mass balance. Such processes are typically diachronous events in restricted basins associated to particular facies of non-surface marine origin or pervasive platform scale diagenetic alteration (Table 1).

Ultimately, most Neoproterozoic comprehensive correlations (for example, Halverson et al., 2005; Walter et al., 2000) are constructed using exclusively $\delta^{13}\text{C}$ variation pattern. In absence of calibrated biostratigraphy (Precambrian) and due to the paucity of radiometric age determinations, these excursions are assumed to be primary in nature and hence globally synchronous. It is important to realize that no independent time chronometer validates the general pattern in Fig. 1 and correlations solely made on $\delta^{13}\text{C}$ variations could be circular (Frauenstein et al., 2009). Considering this paucity of absolute calibration in the Neoproterozoic we propose to use the $^{87}\text{Sr}/^{86}\text{Sr}$ ratio as an independent chronometer to better time constrain these Ediacaran $\delta^{13}\text{C}$ excursions and to test their global coherence and consequently their veracity.

2. $\delta^{13}\text{C}$ excursions

The Ediacaran period $\delta^{13}\text{C}$ record is widely believed to be the witness of three profound negative excursions corresponding to the Marinoan cap carbonates, the Shuram/Wonoka anomaly and the Precambrian/Cambrian boundary (Corsetti and Hagadorn, 2000; Halverson et al., 2005; Jiang et al., 2003a; Knoll et al., 2004; Le Guerroué et al., 2006c). The most profound and enigmatic Shuram/Wonoka anomaly attaining a -12% nadir is repeated in numerous places along correlative strata throughout the basin suggesting a

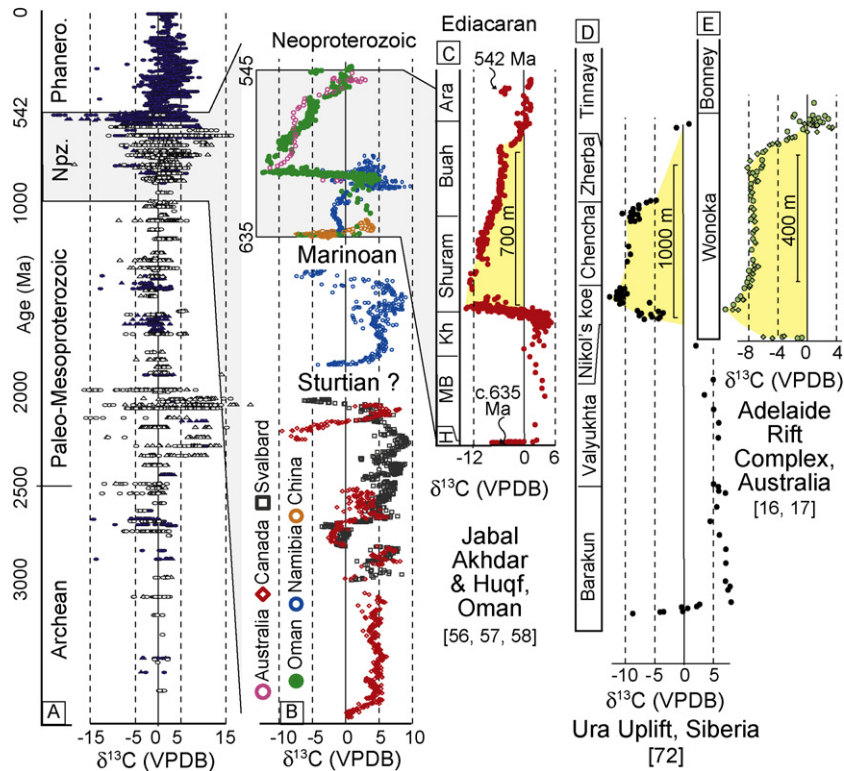


Fig. 1. $\delta^{13}\text{C}$ compilation (A: after (Shields and Veizer, 2002)) throughout Earth history and Neoproterozoic composed from different continental fragments (B: modified from (Halverson et al., 2005)). Note major $\delta^{13}\text{C}$ signal fluctuations during the Neoproterozoic. Detailed Ediacaran $\delta^{13}\text{C}$ record from section in Oman (C (Le Guerroué et al., 2006c)), Siberia (D (Pokrovskii et al., 2006)) and Australia (E (Calver, 2000)). Note pattern reproducibility throughout the thick sedimentary packages but the absence of radiometric or biostratigraphic ages to support definite correlation. Key is H: Hadash; MB: Masirah Bay; Kh: Khufai; Npz: Neoproterozoic; Phanero: Phanerozoic. Oman radiometric age constraints after Bowring et al., 2007.

Fig. 1. Évolution du signal $\delta^{13}\text{C}$ (A : d'après (Shields and Veizer, 2002)) au cours de l'histoire terrestre (et spécifiquement le Néoprotérozoïque), compilée à partir de l'enregistrement sur différents fragments continentaux (B : modifié de (Halverson et al., 2005)). Les fluctuations majeures du signal $\delta^{13}\text{C}$ sont observées au Néoprotérozoïque. Détails de l'enregistrement $\delta^{13}\text{C}$ Édiacarien en Oman (C : (Le Guerroué et al., 2006c)), Sibérie (D : (Pokrovskii et al., 2006)) et Australie (E : (Calver, 2000)). Le signal apparaît reproductible à travers d'épaisses séries sédimentaires, mais aucune contrainte radiométrique ou biostratigraphique ne valide ces corrélations. Légende : H : Hadash ; MB : Masirah Bay ; Kh : Khufai ; Npz : Néoprotérozoïque ; Phanero : Phanérozoïque. Âges radiométriques d'après Bowring et al., 2007.

Table 1

Minimum $^{87}\text{Sr}/^{86}\text{Sr}$ values from literature at the Precambrian/Cambrian boundary (PC-C) and the Marinoan Cap Carbonate stratigraphic interval for individual basin. Data source is in Table S1, Supplementary data. Averaged values allow defining an average Ediacaran trend for $^{87}\text{Sr}/^{86}\text{Sr}$ variation. See discussion in text.

Tableau 1

Valeurs minimales du $^{87}\text{Sr}/^{86}\text{Sr}$ à la limite Précambrienne Cambrienne (PC-C) et de la Cap Carbonate marinoenne, disponible dans la littérature pour chaque bassin. Données originales issues du Tableau S1, Matériel supplémentaire. La moyenne de ces valeurs permet de définir la variation moyenne du $^{87}\text{Sr}/^{86}\text{Sr}$ durant l'Édiacarien. Voir discussion.

	Oman	China	India	Siberia	Australia	Canada	Namibia	Mongolia	Brazil	Average
PC-C values	0.70901	0.70968	0.70950	0.70820	0.70880	No data	0.70852	0.70872	0.70890	0.70891
Cap Carbonate values	0.70842	0.70775	No data	0.70730	No data	0.70732	0.70767	0.70719	0.70744	0.70758
Ediacaran total variation	0.00058	0.00193	-	0.00091	-	-	0.00085	0.00152	0.00146	0.00121
Variation rate per Myr	6.25E-06	2.08E-05	-	9.75E-06	-	-	9.17E-06	1.64E-05	1.57E-05	1.3E-05

primary origin of the values (Burns and Matter, 1993; Cozzi et al., 2004b; Fike et al., 2006; Le Guerroué et al., 2006a; Le Guerroué et al., 2006c). Furthermore detailed studies in the upper Shuram Formation of Oman proved the stratigraphic coherence of -10% $\delta^{13}\text{C}$ values at the scale of a few parasequences (Le Guerroué et al., 2006b), or failed to support a diagenetic overprint (Fike et al., 2006; Le Guerroué

et al., 2006a; Le Guerroué and Cozzi, in press; Le Guerroué and Kennedy, 2007). The Shuram/Wonoka as a primary oceanographic excursion hypothesis is furthermore supported by the presence of large negative excursions located on different continental fragments during the Ediacaran period (Fig. 1, Table S1, Supplementary data). The hypothesis requires a coherent synchronicity of all these potential

equivalent anomalies. To support this, there are, to date, no robust age constraints on any of these excursions, with the exception of the end of the Doushantuo anomaly (China) at ca. 551 Ma (Condon et al., 2005) and subsidence ages on the Shuram Formation of Oman bracketing the excursion between ca. 600 and 550 Ma (Le Guerroué et al., 2006c). Alternatively the Marinoan cap carbonate excursion and the Precambrian/Cambrian boundary are better time constraint by (bio)stratigraphic and/or lithofacies arguments and a few radiometric ages at 635 and 542 Ma respectively (Amthor et al., 2003; Condon et al., 2005; Halverson et al., 2005; Hoffmann et al., 2004; Knoll et al., 2004).

Strongly negative Neoproterozoic $\delta^{13}\text{C}$ excursions (Fig. 1) are currently subject to debate regarding their origin as a primary oceanographic signal (Frauenstein et al., 2009; Le Guerroué and Cozzi, in press). They could imply the oxidation of an extraordinary large dissolved organic carbon reservoir (Fike et al., 2006; Peltier et al., 2007; Rothman et al., 2003) over few millions of years (a few hundred times the duration of the carbon cycle) that is required by the complex stratigraphy of those formations. An organic carbon reservoir oxidation hypothesis for this data has a significant implication for the carbon cycle but however remains a non-steady state reallocation of carbon. It is essential to critically test the global reproducibility and synchronicity of the Shuram/Wonoka to first support a primary excursion hypothesis before attempting robust explanations.

3. Strontium isotopes

The strontium isotope ratio for carbonate rocks reflects the relative contribution of strontium to the ocean from continental weathering and from hydrothermal activity along mid-oceanic ridges (Veizer, 1989). The $^{87}\text{Sr}/^{86}\text{Sr}$ ratio of seawater is very uniform on a global scale, which is an expression of the long oceanic residence time of Sr (3–5 Ma), combined with a relatively short (< 1000 years) oceanic mixing rate (Peterman et al., 1970; Veizer and Compston, 1974). $^{87}\text{Sr}/^{86}\text{Sr}$ is a strong, independent chemostratigraphic tool for making correlations and indirect age assignments especially useful in the Neoproterozoic given the absence of biostratigraphy and paucity of radiometric ages in the fragmentary stratigraphic records (Frauenstein et al., 2009; Halverson et al., 2007; Knoll, 2000; Knoll and Walter, 1992). The general pattern that has emerged for the Neoproterozoic $^{87}\text{Sr}/^{86}\text{Sr}$ curve is one of very low ratios (< 0.7060) early in the era, gradually increasing values in the middle of the Neoproterozoic, and a large monotonic increase to values greater than 0.7085 during the Ediacaran period (Halverson et al., 2007; Prokoph et al., 2008) and references therein. $^{87}\text{Sr}/^{86}\text{Sr}$ data is subject to diagenetic processes but it is not the intention of this manuscript to review the diagenetic overprint of each datasets used here. Readers are referred to original publications where diagenetic issues have been properly addressed. For the purpose of this study, minimum $^{87}\text{Sr}/^{86}\text{Sr}$ values in each set of data are given most credit and it is assumed that they most closely resemble coeval seawater (Frauenstein et al., 2009). The used dataset generally presents Mn/Sr ratio well below 10. $^{87}\text{Sr}/^{86}\text{Sr}$ values are not expected to vary from basin to basin as open

ocean basins largely buffer continental inputs. Variations in dataset are therefore most likely representative of diagenetic interpretation. This issue will be addressed by defining an average Ediacaran trend and apply a correction to each individual basin (see method section).

4. Summary of datasets

4.1. Oman

Oman presents a rather complete stratigraphy (no significant time break is recognized; Fig. 1C) from the deposition of the Hadash Formation cap carbonate Marinoan in age (constrained by detrital zircon population to be < 645 Ma; (Allen, 2007; Bowring et al., 2007; Le Guerroué et al., 2005)) up to the Precambrian/Cambrian boundary recently defined in Oman's subsurface (U/Pb on ash bed (Amthor et al., 2003)). Further detrital zircons populations combined with basinal thermal subsidence analyses constrain the base of the Shuram Formation (~ 600 Ma) and middle Buah Formation baring the end ((~ 550) of the negative $\delta^{13}\text{C}$ Shuram excursion (Le Guerroué et al., 2006c). The isotopic record ($\delta^{13}\text{C}$ and $^{87}\text{Sr}/^{86}\text{Sr}$; Table S1, Supplementary data) is very complete throughout the Ediacaran period and repeated in numerous sections (Fig. 2 (Burns et al., 1994; Burns and Matter, 1993; Cozzi et al., 2004b; Cozzi et al., 2004a; Fike et al., 2006; Le Guerroué et al., 2006b; Le Guerroué et al., 2006a; Le Guerroué et al., 2006c) and references therein). Oman is to date probably the best chemostratigraphically illustrated and completed Ediacaran succession and represents a robust frame to be tested against other worldwide sections.

4.2. China

The Doushantuo Formation of China presents basin wide a quite heterogeneous isotope record bounded by two significant sequence boundaries dissecting the isotope record (see Condon et al., 2005; Ohno et al., 2008; Yang et al., 1999; Zhu et al., 2007 and reference therein). However, the Feidatian–Dongdahe section (Chengjiang, eastern Yunnan province; (Zhu et al., 2007)) records a $\delta^{13}\text{C}$ pattern very similar to the Shuram of Oman. China's negative $\delta^{13}\text{C}$ excursion is constrained to happen during the 551–576 ± 14 Ma period (Chen et al., 2004; Condon et al., 2005) and after 599 ± 4 Ma (Barfod et al., 2002). The overlying Dengying Formation presents the Precambrian/Cambrian boundary associated with a complex Ediacaran fauna (Zhu et al., 2007). Further $^{87}\text{Sr}/^{86}\text{Sr}$ values obtained by Ling et al., 2007 on the Doushantuo and Dengying Formations which are centered around 0.71 are not included in this study as they are much higher than other Ediacaran aged ones (Ling et al., 2007), reflecting potential diagenetic issues, or restriction from the global ocean (Table S1, Supplementary data).

4.3. India

The Krol Formation of the lesser Himalaya of northern India presents a highly variable $\delta^{13}\text{C}$ record (Table S1, Supplementary data (Kaufman et al., 2006)) along its carbonate ramp (Jiang et al., 2002). Only a sparse $^{87}\text{Sr}/^{86}\text{Sr}$

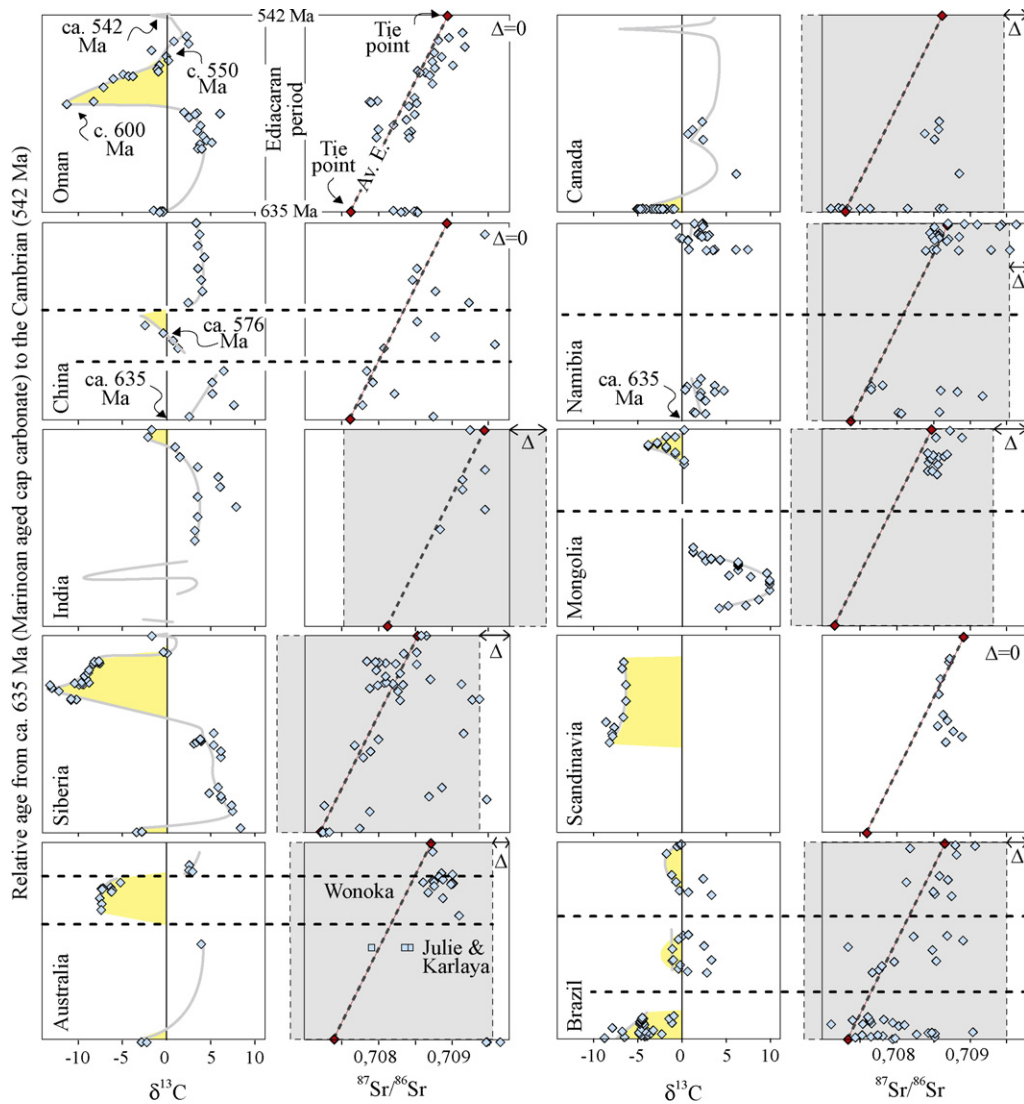


Fig. 2. Chemostratigraphic data ($\delta^{13}\text{C}$ and $^{87}\text{Sr}/^{86}\text{Sr}$; Table 1) for each continental fragment compiled from literature and plotted against calibrated time axis assuming ca. 635 Ma for the cap carbonate and ca. 542 Ma for the Precambrian/Cambrian boundary. Only $\delta^{13}\text{C}$ values associated with $^{87}\text{Sr}/^{86}\text{Sr}$ measurements in similar stratigraphic interval are represented on diagrams. Solid grey line represents the complete available $\delta^{13}\text{C}$ record pattern (includes data points not coupled with $^{87}\text{Sr}/^{86}\text{Sr}$ values). Dashed black line represents well-recognized significant stratigraphic breaks. Radiometric ages are given when available and discussed in the text. Average Ediacaran tie points calculated from all sections (Table 1) are given as well as the average Ediacaran trend that serves as a variation template (dashed grey line: Av. E.). Δ represents the basinal individual $^{87}\text{Sr}/^{86}\text{Sr}$ variation from the average Ediacaran trend. See method section. Note the general rise of $^{87}\text{Sr}/^{86}\text{Sr}$ values throughout the Ediacaran.

Fig. 2. Données chiostratigraphiques ($\delta^{13}\text{C}$ et $^{87}\text{Sr}/^{86}\text{Sr}$; Tableau 1) pour chaque fragment continental. Ces valeurs, issues de la littérature, sont rapportées au temps, considérant un âge de ca. 635 Ma pour la « cap carbonate » et ca. 542 Ma pour la limite Précambrien/Cambrien. Seules les valeurs $\delta^{13}\text{C}$ associées aux valeurs $^{87}\text{Sr}/^{86}\text{Sr}$ dans un même intervalle stratigraphique sont représentées sur ces diagrammes. Les lignes grises représentent l'ensemble de l'enregistrement $\delta^{13}\text{C}$ disponible (incluant les points non couplés à des valeurs $^{87}\text{Sr}/^{86}\text{Sr}$). Les lignes noires pointillées représentent les hiatus stratigraphiques clairement identifiés. Les âges radiométriques fournis sont discutés dans le texte. Les points d'ancrage édiacariens moyens sont calculés à partir de toutes les sections (Tableau 1) et la variation moyenne édiacarienne sert de référence pour l'inter-comparaison (ligne grise pointillée: Av. E.). Δ représente, pour chaque bassin, la variation $^{87}\text{Sr}/^{86}\text{Sr}$ de la moyenne édiacarienne (Av. E.). Voir la partie méthode. Remarquez la croissance générale des valeurs du $^{87}\text{Sr}/^{86}\text{Sr}$ à travers la période édiacarienne.

record is available and limited to the Late Ediacaran and Cambrian period (Table S1, Supplementary data; Krol C to Tal Formation (Tewari and Sial, 2007)). The Krol Formation also contains multiple sequence boundaries potentially biasing the chemostratigraphic record (Jiang et al., 2003b; Jiang et al., 2002).

4.4. Siberia

Siberian sections present a rather matching isotopic pattern with Oman's sections in terms of amplitude and stratigraphic thickness of the negative $\delta^{13}\text{C}$ anomaly and also a large $^{87}\text{Sr}/^{86}\text{Sr}$ dataset (Table S1, Supplementary

data). The $\delta^{13}\text{C}$ excursion is reproduced in different places in the basin and does not present significant unconformities (Fig. 1D (Pokrovskii et al., 2006; Vinogradov et al., 2006a)). The succession is unfortunately not robustly time constrained apart from the presence of a possible Marinoan-aged glacial unit and Cambrian-aged fossils towards the top of the sections (Pokrovskii et al., 2006). Further isotope data is available for the Cambrian and matches worldwide correlations (Vinogradov et al., 2006b; Vinogradov et al., 2006a).

4.5. Australia

The $\delta^{13}\text{C}$ pattern of the Wonoka Formation from the Adelaide Rift Complex of southern Australia matches that of the Shuram Formation of Oman. It is reproduced in different places, spanning a long stratigraphic record (Fig. 1E (Calver, 2000; Calver and Lindsay, 1998; Foden et al., 2001)) with several major stratigraphic unconformities (the Wonoka canyons (Christie-Blick et al., 1990)) that constrain the most negative $\delta^{13}\text{C}$ values (Calver, 2000; Le Guerroué and Kennedy, 2007). $^{87}\text{Sr}/^{86}\text{Sr}$ values from the Julie and Karlaya formations of the Amadeus and officer basins respectively are also included in this data set (Table S1, Supplementary data (Calver and Lindsay, 1998)). Regional studies suggest that the Julie and Karlaya formations correlate to the base of the Wonoka (Calver and Lindsay, 1998). The Australian Ediacaran succession that represents the GSSP is unfortunately not firmly time constrained with the exception of the presence of Ediacaran and Cambrian aged fossils towards the top of the sections.

4.6. Canada

The Windermere Group of western Canada presents a thick Ediacaran succession with very limited $\delta^{13}\text{C}$ measurements available. The strontium isotopes record is restricted to the base of the succession (Table S1, Supplementary data (James et al., 2001; Narbonne et al., 1994)). Stratigraphically, the succession does not appear to contain significant unconformities and strongly resembles the one recorded in Oman (the two “grand cycles” (Allen and Leather, 2006; Le Guerroué et al., 2006c)). If stratigraphic correlations are correct then the negative $\delta^{13}\text{C}$ excursion is not time equivalent to the Shuram anomaly but to the Precambrian/Cambrian shift (Amthor et al., 2003; Corsetti and Hagadorn, 2000). Ultimately, given the paucity of available data, the Shuram excursion could be not yet be documented in western Canada.

4.7. Namibia

The stratigraphic record of Namibia contains a major sedimentary break covering most of the Ediacaran period (Halverson et al., 2005). The lower part of the exposed stratigraphy belongs to the post-Marinoan aged glacial deposits of the Ghaub Formation (Hoffman et al., 1998; Hoffmann et al., 2004) while the upper part belongs to the very end of the Ediacaran period (Fig. 2 (Saylor et al., 1998)). Isotopically (Table S1, Supplementary data (Kauf-

man et al., 1993; Kennedy et al., 1998)), Namibia is probably missing the Shuram anomaly within the unconformity (Halverson et al., 2005).

4.8. Mongolia

The Tsagaan Oloom Formation records, on top of glacial deposits, sediments up to the Cambrian (Brasier et al., 1996b; Shields et al., 1997; Shields et al., 2002). Glacial strata are capped by carbonates presenting a $\delta^{13}\text{C}$ signature typical of “cap carbonate” although the carbonate facies is unusual (Table S1, Supplementary data (Shields et al., 2002)). The succession is not constrained in age and an assignment of the upper Tsagaan glacial diamictite to the Marinoan (c. 635 Ma) could be proposed. This would imply a deposition of the overlying succession within the Ediacaran period. However no Shuram equivalent isotope anomaly is found in Mongolia, instead the $\delta^{13}\text{C}$ record shows highly positive values attaining +10‰ in sequence 3 and 4 (Table S1, Supplementary data). These high values are generally encountered in-between both glacial events (labelled Sturtian-Marinoan (Halverson et al., 2005)) implying than the glacials could be older than 635 Ma. If this hypothesis is correct, a very significant stratigraphic record (the Marinoan glacials and the entire Shuram anomaly) would be missing at top sequence 4 and or 5. Very low strontium isotope ratio supports the assignment of the sequence 3 and 4 to the Sturtian-Marinoan interval (that is generally low (Halverson et al., 2007; Melezhik et al., 2001)). Ediacaran like values are encountered in sequence 5 and 6 with values in unit 5 being more of Lower Ediacaran affinity whereas those one in unit 6 could be of Upper Ediacaran (Table S1, Supplementary data). The end of the section presents a $\delta^{13}\text{C}$ negative excursion inferred to represent the Precambrian/Cambrian boundary (Amthor et al., 2003; Brasier et al., 1996a). We favour the hypothesis that sequence 3 and 4 are pre-Marinoan in age (based on the $\delta^{13}\text{C}$ record). Unit 5 would then represent the base of the Ediacaran period whereas unit 6 would be of Upper Ediacaran age, leading to the Precambrian/Cambrian boundary (Brasier et al., 1996a). This hypothesis is supported by absolute values of the $\delta^{13}\text{C}$ and $^{87}\text{Sr}/^{86}\text{Sr}$ record that also shows significant jump at the sequence boundaries (Fig. 2).

4.9. Scandinavia

The North Central Scandinavian Caledonides presents in its early chemostratigraphic record a negative $\delta^{13}\text{C}$ anomaly (the so-called Leivset marble presenting -8‰ $\delta^{13}\text{C}$ values; Table S1, Supplementary data) on top of a sharp tectonic contact bringing the stratigraphy on top of Silurian aged dark grey marble (Melezhik et al., 2008). If the upper succession is not firmly constrained in time, an Ediacaran age is proposed and largely supported by the $^{87}\text{Sr}/^{86}\text{Sr}$ record (Table S1, Supplementary data); that shows a sharp jump with the underlying Silurian unit (Melezhik et al., 2008)). The anomaly is well reproduced within different sections although it appears incomplete (limited outcrops and fault contact) in regards to the Shuram anomaly (Melezhik et al., 2008).

4.10. Brazil

The succession in Brazil is comprised in the Araras and Alto Paraguai groups (De Alvarenga et al., 2008; De Alvarenga et al., 2004; Nogueira et al., 2007) and is dissected in four different sequences separated by potentially significant time breaks. Brazil's sections present negative $\delta^{13}\text{C}$ values around -2 to -3% all the way up to the Cambrian, contrasting sharply with the pattern observed in Oman or elsewhere (Table S1, Supplementary data). $^{87}\text{Sr}/^{86}\text{Sr}$ ratios support however an Ediacaran age assignment (Table S1, Supplementary data). Yet considering the stratigraphic complexities and possible time missing in the stratigraphic breaks, it is difficult to reconcile a Shuram type anomaly in Brazil.

5. Methods

Available $^{87}\text{Sr}/^{86}\text{Sr}$ values from the literature are used to time calibrate unconstrained pieces of stratigraphy and eventually use the reconstructed time frames to independently test the $\delta^{13}\text{C}$ record. The methodology developed here comprises four steps:

- The Marinoan cap carbonate (ca. 635 Ma (Bowring et al., 2007; Condon et al., 2005; Hoffmann et al., 2004)) and the Precambrian/Cambrian boundary (ca. 542 Ma (Amthor et al., 2003; Knoll et al., 2004)) are defined as two tie points that associated to a $^{87}\text{Sr}/^{86}\text{Sr}$ ratio calculated from averaging minimum values present in all sections (Table 1). These tie points (635 Ma; 0.70758) and (542 Ma; 0.70891) are chosen as they are time equivalent and easily recognizable in all sections. Our values are in a close range to Halverson et al. (Halverson et al., 2007). The slight difference being non relevant here as these tie points are used for comparison among

datasets used here. Theoretical $^{87}\text{Sr}/^{86}\text{Sr}$ variation between the two tie points is around 0.00121 (Table 1) and is assumed constant through time. This assumption is largely supported by individual dataset that presents a rather linear variation and previous comprehensive studies that fail to identify first order knee points in the Ediacaran period (Table S1, Supplementary data (Halverson et al., 2007; Prokoph et al., 2008) and references therein);

- The steady variation between the two tie points represents the theoretical global ocean variation throughout the Ediacaran and serves as a template to compare and calibrate individual datasets. Variation in $^{87}\text{Sr}/^{86}\text{Sr}$ among individual datasets exists and reflects basinal individual specificities related to diagenetic alteration. Individual datasets are therefore corrected for variation from the average global Ediacaran trend by shifting their entire dataset to lower or higher $^{87}\text{Sr}/^{86}\text{Sr}$ values. This is Δ on Fig. 2. This correction is applied here in order to allow datasets comparison, it is not assumed to represent specific geological phenomenon;
- Fig. 2 is constructed using chemostratigraphic data from the literature (Table S1, Supplementary data) given available biostratigraphic record, recognized sedimentary hiatuses and absolute radiometric constraints. Stratigraphic pieces belonging to the cap carbonate sequence are bounded to the 635 Ma lower limits and strata containing the Precambrian/Cambrian boundary sequence are bounded to the 542 Ma upper limits. Time unconstrained pieces of stratigraphy, such as strata bounded by major regional unconformities are time calibrated (moved along the time axis) by nearest match of their $^{87}\text{Sr}/^{86}\text{Sr}$ values (corrected for local basin setting (Δ)) with the average Ediacaran trend. Since diagenesis increases $^{87}\text{Sr}/^{86}\text{Sr}$ ratio, data points are not individually time adjusted. Minimum $^{87}\text{Sr}/^{86}\text{Sr}$ values of stratigraphic

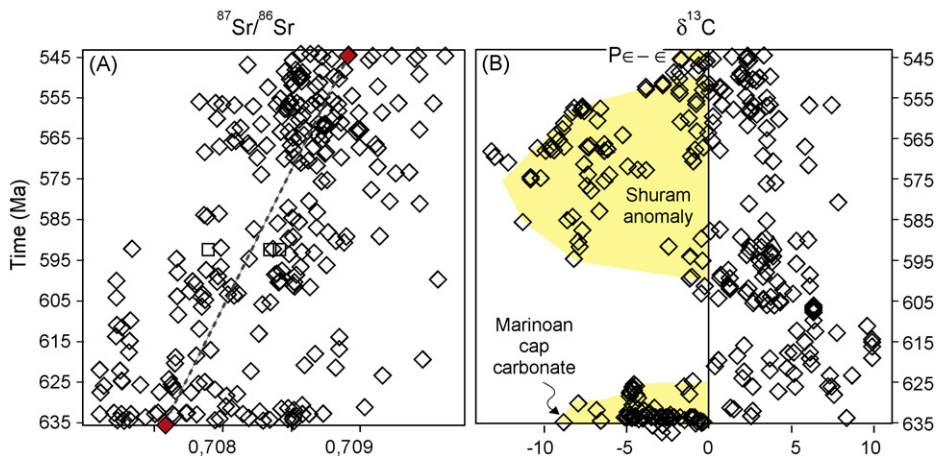


Fig. 3. Ediacaran $^{87}\text{Sr}/^{86}\text{Sr}$ (A) and $\delta^{13}\text{C}$ (B) composite constructed using time frame defined in Fig. 2. Note the 3 distinctive negative $\delta^{13}\text{C}$ packages corresponding to the Marinoan cap carbonates, the Precambrian/Cambrian boundary (PC-C) and the Shuram anomaly (yellow areas). $^{87}\text{Sr}/^{86}\text{Sr}$ tie points (red point) defined in Table 1 are represented as well as the average Ediacaran trend (dashed grey line). Note that the bulk of negative $\delta^{13}\text{C}$ values associated with the Shuram anomaly start around 600 Ma and end around 550 Ma. See discussion in text.

Fig. 3. Composites $^{87}\text{Sr}/^{86}\text{Sr}$ (A) et $\delta^{13}\text{C}$ (B) édiacariens, construits en utilisant l'échelle de temps définie en Fig. 2. Les 3 paquets $\delta^{13}\text{C}$ négatifs très distincts correspondent à la cap carbonate marinoenne, à la limite Précambrien/Cambrien (PC-C) et à l'anomalie de Shuram (zone jaune). Les points d'ancrage $^{87}\text{Sr}/^{86}\text{Sr}$ (points rouges) définis dans le Tableau 1 sont aussi représentés, ainsi que la moyenne édiacarienne (ligne grise pointillée). L'essentiel des valeurs $\delta^{13}\text{C}$ négatives sont associées à l'anomalie de Shuram commençant autour de 600 Ma et finissant vers 550 Ma. Voir discussion dans le texte.

fragments are calibrated as coherent block. This procedure is supported by the large residence time of Sr in the ocean (3–5 Ma);

- Finally the $\delta^{13}\text{C}$ values are stacked (Fig. 3B) using the time calibration reconstructed from $^{87}\text{Sr}/^{86}\text{Sr}$ values in Fig. 2. It is important to note that the time calibration is constructed entirely without reference to $\delta^{13}\text{C}$ curve. Only samples with both $^{87}\text{Sr}/^{86}\text{Sr}$ and $\delta^{13}\text{C}$ measurements at a strictly similar stratigraphic interval are used (Fig. 2).

6. Results

With current published isotope data, absolute age constraints, acceptance of minimum diagenetic modification to values, and the use of the $^{87}\text{Sr}/^{86}\text{Sr}$ steady rising trend to independently calibrate poorly time constrained fragments, the Ediacaran period provides a compelling example of stratigraphic consistency of carbon isotope values between sections. In the light of this approach, the reconstruction shows that 3 individual negative $\delta^{13}\text{C}$ packages appear in the Ediacaran composite record (Fig. 3). These negative $\delta^{13}\text{C}$ anomalies are well reproduced and have duration and amplitude specificities. They correspond to:

- (1) the well established Marinoan cap carbonate anomaly immediately preceding the glacial deposits (Halverson et al., 2005; Hoffman et al., 1998; Shields, 2005);
- (2) a long lived and profound Shuram/Wonoka excursion (Condon et al., 2005; Halverson et al., 2005; Le Guerroué et al., 2006c; Melezhik et al., 2008);
- (3) the Precambrian/Cambrian boundary shift (Amthor et al., 2003; Corsetti and Hagadorn, 2000; Saylor et al., 1998).

This composite record fails to recognize, at the global scale, other potential negative $\delta^{13}\text{C}$ excursions such as the one present in the lower stratigraphy of the Krol Formation of India. Such excursions are therefore interpreted as non-synchronous and are probably related to diagenetic issues or basinal disconnection from the global ocean.

The bulk of the negative values associated with the Shuram/Wonoka excursion start around 600 Ma and end somewhere around 550 Ma (Fig. 3). These brackets are supported by published ages constraining the nadir of the excursion in Oman and China (Barfod et al., 2002; Le Guerroué et al., 2006c) as well as a ca. 551 Ma constraining the end of the anomaly in China (Condon et al., 2005). Other authors (Bowring et al., 2007; Condon et al., 2005; Fike et al., 2006; Halverson et al., 2007) favour a much younger age for the nadir of the Shuram excursion although no direct radiometric age supports these assignments. The anomaly appears to last 40–50 Ma; this very long duration is well supported by sections like those in Oman and Siberia, whereas sections like those of Australia and China suggest a shorter duration around 20–30 Ma (Fig. 3). It is also to note the partial time overlap of positive or weakly negative $\delta^{13}\text{C}$ values during the Shuram anomaly probably due to inherent flaws in the time reconstruction and the lack of data point in some of the

datasets. This is particularly the case in the Brazilian and Canadian sections. However Canada seriously lack data in this very specific interval and the nearly continuous $\delta^{13}\text{C}$ record in Brazil with values around 0‰ not easily reconcilable with the general trend.

7. Discussion

It is important to realize that there is no common mechanism driving the $^{87}\text{Sr}/^{86}\text{Sr}$ and $\delta^{13}\text{C}$ record and that standard screenings failed to identify major diagenetic overprinting. Diagenesis generally raises Mn contents and $^{87}\text{Sr}/^{86}\text{Sr}$ ratios and lowers Sr contents and $\delta^{13}\text{C}$ as well as $\delta^{18}\text{O}$ values of carbonate (Brand and Veizer, 1980; Veizer, 1983), also carbonates with Mn/Sr < 10 more often retain primary carbon isotope compositions (Derry et al., 1992; Kaufman et al., 1993; Kaufman and Knoll, 1995), while carbonate with Mn/Sr > 10 and $\delta^{18}\text{O} > -10\text{‰}$ may exhibit altered C-isotope compositions. Isotopic data used here were screened in original publication and the reader is referred to originally published material for further discussion on diagenetic screening of individual data sets that all pass these standard assessments.

Given the large (3–5 Ma) residence time of Sr in the ocean this study focuses on minimum $^{87}\text{Sr}/^{86}\text{Sr}$ values (closest to past coeval oceanic composition) of coherent stratigraphic fragments allowing to overcome diagenetic overprint of specific horizons. The basinal correction (Δ on Fig. 2; see method section) from the averaged Ediacaran trend (Table 1) allows compensating for variation in datasets and best time calibrate all sections. These variations are likely to represent after deposition diagenesis, shifting values throughout individual basin. Another hypothesis would be a diachronic nature of the cap carbonate tie point. This appears less likely as the cap carbonate is synchronous on two continental fragments (Condon et al., 2005; Hoffmann et al., 2004) and probably a third (Bowring et al., 2007).

The Ediacaran $^{87}\text{Sr}/^{86}\text{Sr}$ composite record obtained is in good agreement with past studies (Halverson et al., 2007; Jacobsen and Kaufman, 1999; Thomas et al., 2004; Walter et al., 2000) although datasets from individual basin show some variation (Fig. 3A). The composite section on Fig. 3B shows a rise from about 0.707 to 0.7085 throughout the Ediacaran period without individual basinal correction (Δ on Fig. 2). Ediacaran average variation is in the order of 0.00121 from the cap carbonate to the Precambrian/Cambrian boundary tie points (Table 1) with a rise of about $1.30 \times 10^{-5}/\text{Ma}$ that is comparable to the $^{87}\text{Sr}/^{86}\text{Sr}$ variation throughout the Cretaceous period based on Prokoph et al., 2008 compilation (their Fig. 4, shows a variation in the order of $1.0 \times 10^{-5}/\text{Ma}$ in the Cretaceous). Classically the Ediacaran large-scale steady variation is interpreted to be the record of the final stage of the Rodinia breakup and the early amalgamation of Gondwana during the Ediacaran (Halverson et al., 2007). The slow variation in the Ediacaran $^{87}\text{Sr}/^{86}\text{Sr}$ record could be the witness of this tectonically (erosion rate related) more quiescent period.

It should be noted from Fig. 3B, that the absence of such a distinctive $\delta^{13}\text{C}$ long-lived feature in Canada (all positive values (Narbonne et al., 1994)) and Brazil (all negative

values (De Alvarenga et al., 2008; De Alvarenga et al., 2004; Nogueira et al., 2007)), and the partial time overlap of positive values in South China (Condon et al., 2005), but see Zhu et al., 2007 and India (that is extremely variable (Kaufman et al., 2006)), argues against a global feature.

Studying these basins in greater detail and chemostratigraphic resolution will help clarify inconsistencies. For example, the Johnny Formation of Death Valley (Corsetti and Kaufman, 2003) and Windermere Group of Canada (Narbonne et al., 1994) excursions are based on <30 values from up to 2000 m of section. Identification of possible significant time break biasing the chemostratigraphic record as well as potential basin restriction from the global ocean needs to be clarified in all successions. For example the *Doushantuo* Formation has recently been interpreted to be locally deposited in an alkaline lake (Bristow et al., 2009) and probably stratified water column (Ader et al., 2009). Recent improvement in the Ediacaran biostratigraphy (Grey and Calver, 2007; Shen et al., 2008; Willman and Moczydlowska, 2008) and paleogeography (Li et al., 2008; Pisarevsky et al., 2008) will help resolving uncertainties and refine the chronostratigraphic record.

Ultimately, a demonstrated synchronicity of the Shuram anomaly equivalent excursions on all continental fragments is a fundamental step towards understanding its origin as a primary oceanographic phenomenon. A non-coeval interpretation will clearly point out to diagenetic alteration of the carbonate material and furthermore questions Neoproterozoic global correlation mainly reconstructed from the $\delta^{13}\text{C}$ record (Halverson et al., 2005; Knoll et al., 2004).

8. Conclusions

The study of different Ediacaran aged $^{87}\text{Sr}/^{86}\text{Sr}$ record of several continental masses leads to the following conclusions:

- A $\delta^{13}\text{C}$ excursion of the magnitude and duration of the Shuram/Wonoka anomaly, if representative of a primary oceanographic signal, should be coeval in different sections on different continental margins. Indeed it has to be repeated everywhere connected to the global ocean to rule out diachronous diagenetic imprints. Correlations solely based on the sparse available radiometric ages are currently not able to address robustly the synchronicity issue.
- This study proposes a critical test of this hypothesis by using strontium isotopes as an independent chronometer to better time constrain individual pieces of Ediacaran stratigraphy that otherwise only relies on a few, often weak, radiometric age constraints. This new composite section validates the Shuram/Wonoka excursion reproducibility and synchronicity at the global scale and proposes a negative $\delta^{13}\text{C}$ shift reaching a nadir $> -10\%$ around 600 Ma and followed by a steady recovery towards positive values ending around 550 Ma. This negative excursion is recorded in many different basins on several continental fragments (Oman, Australia, Siberia, China, Scandinavia) supporting its origin as a primary oceanographic signal.

- The Shuram/Wonoka excursion is a secular phenomenon spanning a few tens of millions of years and is therefore representative of the changing global ocean value in steady state condition. The exogenic cycle must have functioned with very different, and currently unrecognized, controls than during the Phanerozoic (Bartley and Kah, 2004) probably involving a large carbon reservoir with much longer residence time (Rothman et al., 2003) or a protracted release of significant light carbon. The strongly negative $\delta^{13}\text{C}$ excursions (Fig. 1) could imply oxidation of such a large reservoir of organic carbon (Fike et al., 2006; Peltier et al., 2007; Rothman et al., 2003). A primary marine interpretation for this data has significant implications for the interrelationship of evolutionary events and the carbon cycle that has not been fully explored (Peltier et al., 2007) and could record oxidation of this organic carbon reservoir with draw down of atmospheric oxygen. The end of the oxidation event around 550 Ma would allow $p\text{O}_2$ to build up sufficiently to impact metazoan evolution.

Acknowledgements

Swiss national research project (Number: PBEZ2-115170) is thanked for financial support. Petroleum Development Oman and especially Jan Schreurs are thanked for long time support. This is a contribution to the IGCP-512 project. Anonymous reviewers helped to improve the manuscript.

Appendix A. Supplementary data

Supplementary data associated with this article can be found, in the online version, at doi:10.1016/j.crte.2009.12.008.

References

- Ader, M., Macouin, R.I.F., Trindade, M.-H., Hadrien, Z., Yang, Z., Sun, and J. Besse. 2009. A multilayered water column in the Ediacaran Yangtze platform? Insights from carbonate and organic matter paired $\delta^{13}\text{C}$. *Earth and Planetary Science Letters* 288, no. 1–2 (October 30): 213–227. doi:10.1016/j.epsl.2009.09.024. <http://www.sciencedirect.com/biblioplans.gate.inist.fr/science/article/B6V61-4XFF2S3-3/2/77567be090b7a993ee1a6bf55dae9149..>
- Allen, P.A., 2007. The Huqf Supergroup of Oman: Basin development and context for Neoproterozoic glaciation. *Earth-Science Reviews* 84, 139–185.
- Allen, P.A., Leather, J., 2006. Post-Marinoan marine siliciclastic sedimentation: The Masirah Bay Formation, Neoproterozoic Huqf Supergroup of Oman. *Precamb. Res.* 144, 167–198.
- Amthor, J.E., Grotzinger, S., Schröder, S.A., Bowring, J., Ramezani, M., Martin, M., Matter, A., 2003. Extinction of *Cloudina* and *Namacalathus* at the Precambrian-Cambrian boundary in Oman. *Geology* 31, 431–434.
- Anbar, A.D., Knoll, A.H., 2002. Proterozoic ocean chemistry and evolution: A bioinorganic bridge? *Science* 297, 1137–1142.
- Barfod, H.G., Albarède, F., Knoll, A.H., Xiao, S., Télouk, P., Frei, R., Baker, J., 2002. New Lu-Hf and Pb-Pb age constraints on the earliest animal fossils. *Earth Planet Sci. Lett.* 201, 203–212.
- Bartley, J.K., Kah, L.C., 2004. Marine carbon reservoir, $\text{C}_{\text{org}}-\text{C}_{\text{carb}}$ coupling, and the evolution of the Proterozoic carbon cycle. *Geology* 32, 129–132.
- Bowring, S.A., Grotzinger, J.P., Condon, D.J., Ramezani, J., Newall, M.J., Allen, P.A., 2007. Geochronologic constraints on the chronostratigraphic framework of the Neoproterozoic Huqf Supergroup, Sultanate of Oman. *Am. J. Sci.* 307, 1097–1145.
- Brand, U., Veizer, J., 1980. Chemical diagenesis of a multicomponent carbonate system; 1, Trace elements. *J. Sedim. Res.* 50, 1219–1236.

- Brasier, M.D., Dorjnamjaa, D., Lindsay, J.F., 1996a. The Neoproterozoic to Early Cambrian in Southwest Mongolia; an introduction. *Geol. Mag.* 133, 365–369.
- Brasier, M.D., Shields, G., Kuleshov, V.N., Zhegallo, E.A., 1996b. Integrated chemo- and biostratigraphic calibration of early animal evolution; Neoproterozoic–Early Cambrian of Southwest Mongolia. *Geol. Mag.* 133, 445–485.
- Bristow, T.F., Kennedy, M.J., Derkowski, A., Droser, M.L., Jiang, G., Creaser, R.A., 2009. Mineralogical constraints on the paleoenvironments of the Ediacaran Doushantuo Formation. In: *Proceedings of the National Academy of Sciences*, 106. pp. 13190–13195.
- Broecker, W.S., Peng, T.H., 1982. *Tracers in the Sea*. Eldigio Press, Palisades, New York, 690 p.
- Burns, S.J., Matter, A., 1993. Carbon isotopic record of the Latest Proterozoic from Oman. *Eclogae Geol. Helv.* 86, 595–607.
- Burns, S.J., Haudenschild, U., Matter, A., 1994. The strontium isotopic composition of carbonates from the Late Precambrian (~560–540 Ma) Huqf Group of Oman. *Chem. Geol.* 111, 269–282.
- Calver, C.R., 2000. Isotope stratigraphy of the Ediacaran (Neoproterozoic III) of the Adelaide Rift Complex, Australia, and the overprint of water column stratification. *Precamb. Res.* 100, 121–150.
- Calver, C.R., Lindsay, J.F., 1998. Ediacarian sequence and isotope stratigraphy of the Officer Basin, South Australia. *Austr. J. Earth Sci.* 45, 513–532.
- Canfield, D.E., Teske, A., 1996. Late Proterozoic rise in atmospheric oxygen concentration inferred from phylogenetic and sulphur-isotope studies. *Nature* 382, 127–132.
- Chen, D.F., Dong, W.Q., Zhu, B.Q., Chen, X.P., 2004. Pb–Pb ages of Neoproterozoic Doushantuo phosphorites in South China: Constraints on early metazoan evolution and glaciation events. *Precamb. Res.* 132, 123–132.
- Christie-Blick, N., von der Borch, C.C., DiBona, P.A., 1990. Working hypotheses for the origin of the Wonoka Canyons (Neoproterozoic), South Australia. *Am. J. Sci.* 290, 295–332.
- Condon, D., Zhu, M., Bowring, S., Wang, W., Yang, A., Jin, Y., 2005. U–Pb Ages from the Neoproterozoic Doushantuo Formation, China. *Science* 308, 95–98.
- Corsetti, F.A., Hagadorn, J.W., 2000. Precambrian–Cambrian transition: Death Valley, United States. *Geology* 28, 299–302.
- Corsetti, F.A., Kaufman, A.J., 2003. Stratigraphic investigations of carbon isotope anomalies and Neoproterozoic ice ages in Death Valley, California. *Geol. Soc. Am. Bull.* 115, 916–932.
- Cozzi, A., Grotzinger, J.P., Allen, P.A., 2004a. Evolution of a terminal Neoproterozoic carbonate ramp system (Buah Formation, Sultanate of Oman): Effects of basement paleotopography. *Geol. Soc. Am. Bull.* 116, 1121–1131.
- Cozzi, A., Allen, P.A., Grotzinger, J.P., 2004b. Understanding carbonate ramp dynamics using $\delta^{13}\text{C}$ profiles: Examples from the Neoproterozoic Buah Formation of Oman. *Terra Nova* 16, 62–67.
- De Alvarenga, C.J.S., Santos, R.V., Dantas, E.L., 2004. C–O–Sr isotopic stratigraphy of cap carbonates overlying Marinoan-age glacial diamictites in the Paraguay Belt, Brazil. *Precamb. Res.* 131, 1–21.
- De Alvarenga, C.J.S., Dardenne, M.A., Santos, R.V., Brod, E.R., Gioia, S.M.C.L., Sial, A.N., Dantas, E.L., Ferreira, V.P., 2008. Isotope stratigraphy of Neoproterozoic cap carbonates in the Araras Group, Brazil. *Gondwana Research* 13, 469–479.
- Derry, L.A., Kaufman, A.J., Jacobsen, S.B., 1992. Sedimentary cycling and environmental change in the Late Proterozoic: Evidence from stable and radiogenic isotopes. *Geochim. Cosmochim. Acta* 56, 1317–1329.
- Fike, D.A., Grotzinger, J.P., Pratt, L.M., Summons, R.E., 2006. Oxidation of the Ediacaran Ocean. *Nature* 444, 744–747.
- Foden, J., Barovich, K., Jane, M., O'Halloran, G., 2001. Sr-isotope evidence for Late Neoproterozoic rifting in the Adelaide Geosyncline at 586 Ma: Implications for a Cu ore forming fluid flux. *Precamb. Res.* 106, 291–308.
- Frauenstein, F., Veizer, J., Beukes, N., Van Niekerk, H.S., Coetzee, L.L., Transvaal Supergroup carbonates: Implications for Paleoproterozoic $\delta^{18}\text{O}$ and $\delta^{13}\text{C}$ records. *Precamb. Res.* In press.
- Grey, K., Calver, C.R., 2007. Ediacaran oxidation and biotic evolution. *Nature* 450, E17–E117.
- Halverson, G.P., Dudas, F.O., Maloof, A.C., Bowring, S.A., 2007. Evolution of the $^{87}\text{Sr}/^{86}\text{Sr}$ composition of Neoproterozoic seawater. *Palaeogeogr. Palaeoclimatol. Palaeoecol.* 256, 103–129.
- Halverson, G.P., Hoffman, P.F., Schrag, D.P., Maloof, A.C., Rice, A.H.N., 2005. Towards a Neoproterozoic composite carbon isotope record. *Geol. Soc. Am. Bull.* 117, 1181–1207.
- Hayes, J.M., Strauss, H., Kaufman, A.J., 1999. The abundance of ^{13}C in marine organic matter and isotopic fractionation in the global biogeochemical cycle of carbon during the past 800 Ma. *Chem. Geol.* 161, 103–125.
- Hoffman, P.F., Kaufman, A.J., Halverson, G.P., Schrag, D.P., 1998. A Neoproterozoic snowball Earth. *Science* 281, 1342–1346.
- Hoffmann, K.H., Condon, D.J., Bowring, S.A., Crowley, J.L., 2004. U–Pb zircon date from the Neoproterozoic Ghaub Formation, Namibia: Constraints on Marinoan glaciation. *Geology* 32, 817–820.
- Jacobsen, S.B., Kaufman, A.J., 1999. The Sr, C and O isotopic evolution of Neoproterozoic seawater. *Chem. Geol.* 161, 37–57.
- James, N.P., Narbonne, G.M., Kyser, T.K., 2001. Late Neoproterozoic cap carbonates: Mackenzie Mountains, northwestern Canada: Precipitation and global glacial meltdown. *Canad. J. Earth Sci.* 38, 1229–1262.
- Jiang, G., Kennedy, M.J., Christie-Blick, N., 2003a. Stable isotopic evidence for methane seeps in Neoproterozoic postglacial cap carbonates. *Nature* 426, 822–826.
- Jiang, G., Christie-Blick, N., Kaufman, A.J., Banerjee, D.M., Rai, V., 2003b. Carbonate platform growth and cyclicity at a terminal Proterozoic passive margin, Infra Krol Formation and Krol Group, Lesser Himalaya, India. *Sedimentology* 50, 921–952.
- Jiang, G.Q., Christie-Blick, N., Kaufman, A.J., Banerjee, D.M., Rai, V., 2002. Sequence stratigraphy of the Neoproterozoic Infra Krol Formation and Krol Group, Lesser Himalaya, India. *J. Sedim. Res.* 72, 524–542.
- Kah, L.C., Lyons, T.W., Frank, T.D., 2004. Low marine sulphate and protracted oxygenation of the Proterozoic biosphere. *Nature* 431, 834–838.
- Kaufman, A.J., Knoll, A.H., 1995. Neoproterozoic variations in the C isotopic composition of seawater: Stratigraphic and biogeochemical implications. *Precamb. Res.* 73, 27–49.
- Kaufman, A.J., Jacobsen, S.B., Knoll, A.H., 1993. The Vendian record of Sr and C isotopic variations in seawater: Implications for tectonics and palaeoclimate. *Earth Planet. Sci. Lett.* 120, 409–430.
- Kaufman, A.J., Jiang, G., Christie-Blick, N., Banerjee, D.M., Rai, V., 2006. Stable isotope record of the terminal Neoproterozoic Krol platform in the Lesser Himalayas of northern India. *Precamb. Res.* 147, 156–185.
- Kennedy, M., Droser, M., Mayer, L.M., Pevear, D., Mrofk, D., 2006. Late Precambrian Oxygenation; Inception of the Clay Mineral Factory. *Science* 311, 1446–1449.
- Kennedy, M.J., Runnegar, B., Prave, A.R., Hoffmann, K.H., Arthur, M.A., 1998. Two or four Neoproterozoic glaciations? *Geology* 26, 1059–1063.
- Knoll, A.H., 2000. Learning to tell Neoproterozoic time. *Precamb. Res.* 100, 3–20.
- Knoll, A.H., Walter, M.R., 1992. Latest Proterozoic stratigraphy and Earth history. *Nature* 356, 673–677.
- Knoll, A.H., Carroll, S.B., 1999. Early Animal Evolution: Emerging Views from Comparative Biology and Geology. *Science* 284.
- Knoll, A.H., Walter, M.R., Narbonne, G.M., Christie-Blick, N., 2004. A New Period for the Geologic Time Scale. *Science* 305, 621–622.
- Knoll, A.H., Hayes, J.M., Kaufman, A.J., Swett, K., Lambert, I.B., 1986. Secular variation in carbon isotope ratios from Upper Proterozoic successions of Svalbard and East Greenland. *Nature* 321, 832–838.
- Le Guerroué, E., Kennedy, M., 2007. Neoproterozoic Carbon Isotopes of the Neoproterozoic Shuram and Wonoka Formations., AAPG Annual Convention and Exhibition. Long Beach, California. (April 1–4 2007). Technical Program.
- Le Guerroué, E., Cozzi, A., Veracity of Neoproterozoic negative C isotope values: The termination of the Shuram negative excursion, Gondwana Research. In press.
- Le Guerroué, E., Allen, P.A., Cozzi, A., 2005. Two distinct glacial successions in the Neoproterozoic of Oman. *GeoArabia* 10, 17–34.
- Le Guerroué, E., Allen, P.A., Cozzi, A., 2006a. Chemostratigraphic and sedimentological framework of the largest negative carbon isotopic excursion in Earth history: The Neoproterozoic Shuram Formation (Nafun Group, Oman). *Precamb. Res.* 146, 68–92.
- Le Guerroué, E., Allen, P.A., Cozzi, A., 2006b. Parasequence development in the Ediacaran Shuram Formation (Nafun Group, Oman): High resolution stratigraphic test for primary origin of negative carbon isotopic ratios. *Basin Res.* 18, 205–220.
- Le Guerroué, E., Allen, P.A., Cozzi, A., Etienne, J.L., Fanning, C.M., 2006c. 50 Myr recovery from the largest negative $\delta^{13}\text{C}$ excursion in the Ediacaran ocean. *Terra Nova* 18, 147–153.
- Li, Z.X., Bogdanova, S.V., Collins, A.S., Davidson, A., De Waele, B., Ernst, R.E., Fitzsimons, I.C.W., Fuck, R.A., Gladkochub, D.P., Jacobs, J., Karlstrom, K.E., Lu, S., Natapov, L.M., Pease, V., Pisarevsky, S.A., Thrane, K., Vernikovsky, V., 2008. Assembly, configuration, and break-up history of Rodinia: A synthesis. *Precamb. Res.* 160, 179–210.
- Ling, H.-F., Feng, H.-Z., Pan, J.-Y., Jiang, S.-Y., Chen, Y.-Q., Chen, X., 2007. Carbon isotope variation through the Neoproterozoic Doushantuo and Dengying Formations, South China: Implications for chemostratigraphy and paleoenvironmental change. *Palaeogeogr. Palaeoclimatol. Palaeoecol.* 254, 158–174.

- Magaritz, M., 1991. Carbon isotopes, time boundaries and evolution. *Terra Nova* 3, 251–256.
- Melezhik, V.A., Gorokhov, I.M., Kuznetsov, A.B., Fallick, A.E., 2001. Chemostratigraphy of Neoproterozoic carbonates: Implications for 'blind' dating. *Terra Nova* 13, 1–11.
- Melezhik, V.A., Roberts, D., Fallick, A.E., Gorokhov, I.M., 2008. The Shuram-Wonoka event recorded in a high-grade metamorphic terrane: Insight from the Scandinavian Caledonides. *Geol. Mag.* 145, 161–172.
- Narbonne, G.M., 1994. New Ediacaran Fossils from the Mackenzie Mountains, Northwestern Canada. *J. Paleontology* 68, 411–416.
- Narbonne, G.M., Kaufman, A.J., Knoll, A.H., 1994. Integrated chemostratigraphy and biostratigraphy of the Windermere Supergroup, northwestern Canada; implications for Neoproterozoic correlations and the early evolution of animals; with Suppl. Data 9434. *Geol. Soc. Am. Bull.* 106, 1281–1292.
- Nogueira, A.C.R., Riccomini, C., Sial, A.N., Moura, C.A.V., Trindade, R.I.F., Fairchild, T.R., 2007. Carbon and strontium isotope fluctuations and paleoceanographic changes in the Late Neoproterozoic Araras carbonate platform, southern Amazon craton. *Brazil Chem. Geol.* 237, 168–190.
- Ohno, T., Komiya, T., Ueno, T.H.Y., Maruyama, S., 2008. Determination of $^{88}\text{Sr}/^{86}\text{Sr}$ mass-dependent isotopic fractionation and radiogenic isotope variation of $^{87}\text{Sr}/^{86}\text{Sr}$ in the Neoproterozoic Doushantuo Formation. *Gondwana Res.* 14, 126–133.
- Peltier, W.R., Liu, Y., Crowley, J.W., 2007. Snowball Earth prevention by dissolved organic carbon remineralization. *Nature* 450, 813–818.
- Peterman, Z.E., Hedge, C.E., Tourtelot, H.A., 1970. Isotopic composition of strontium in sea water throughout Phanerozoic time. *Geochim. Cosmochim. Acta* 34, 105–120.
- Pisarevsky, S.A., Murphy, J.B., Cawood, P.A., Collins, A.S., 2008. Late Neoproterozoic and Early Cambrian palaeogeography: Models and problems. *Geological Society, London. Special Publications* 294, 9–31.
- Pokrovskii, B.G., Melezhik, V.A., Bujakaite, M.I., 2006. Carbon, Oxygen, Strontium, and Sulfur isotopic compositions in Late Precambrian rocks of the Patom Complex, central Siberia: Communication 1. results, isotope stratigraphy, and dating problems. *Lithology Mineral Resources* 41, 450–474.
- Prokoph, A., Shields, G.A., Veizer, J., 2008. Compilation and time-series analysis of a marine carbonate $\delta^{18}\text{O}$, $\delta^{13}\text{C}$, $^{87}\text{Sr}/^{86}\text{Sr}$ and $\delta^{34}\text{S}$ database through Earth history. *Earth-Sci. Rev.* 87, 113–133.
- Rothman, D.H., Hayes, J.M., Summons, R.E., 2003. Dynamics of the Neoproterozoic carbon cycle. In: *Proceedings of the National Academy of Sciences USA*, 10, pp. 8124–8129.
- Saylor, B.Z., Kaufman, A.J., Grotzinger, J.P., Urban, F., 1998. A composite reference section for terminal Proterozoic strata of southern Namibia. *J. Sedim. Res.* 68, 1223–1235.
- Schidlowski, M., Aharon, P., 1992. Carbon cycle and carbon isotope record: Geochemical impact of life over 3.8 Ga of Earth history. In: Schidlowski, M. (Ed.), *Early Organic Evolution: Implications of Mineral and Energy Resources*. Springer, Berlin, pp. 147–175.
- Shen, Y., Zhang, T., Hoffman, P.F., 2008. On the coevolution of Ediacaran oceans and animals. In: *Proceedings of the National Academy of Sciences*, 105, pp. 7376–7381.
- Shields, G.A., 2005. Neoproterozoic cap carbonates: A critical appraisal of existing models and the plume world hypothesis. *Terra Nova* 17, 299–310.
- Shields, G., Veizer, J., 2002. Precambrian marine carbonate isotope database: Version 1.1. *Geochemistry Geophysics Geosystems* 3, 1031.
- Shields, G., Stille, P., Brasier, M.D., Atudorei, N.-V., 1997. Stratified oceans and oxygenation of the late Precambrian environment: A post glacial geochemical record from the Neoproterozoic of W. Mongolia. *Terra Nova* 9, 218–222.
- Shields, G.A., Brasier, M.D., Stille, P., Dorjnamjaa, D.-i., 2002. Factors contributing to high ^{13}C values in Cryogenian limestones of western Mongolia. *Earth Planet. Sci. Lett.* 196, 99–111.
- Swart, P.K., Eberli, G., 2005. The nature of the $\delta^{13}\text{C}$ of periplatform sediments: Implications for stratigraphy and the global carbon cycle. *Sedim. Geol.* 175, 115–129.
- Tevari, V.C., Sial, A.N., 2007. Neoproterozoic-Early Cambrian isotopic variation and chemostratigraphy of the Lesser Himalaya, India, Eastern Gondwana. *Chem. Geol.* 237, 64–88.
- Thomas, C., Graham, C., Ellam, R., Fallick, A., 2004. $^{87}\text{Sr}/^{86}\text{Sr}$ chemostratigraphy of Neoproterozoic Dalradian limestones of Scotland and Ireland: Constraints on depositional ages and time scales. *J. Geol. Soc.* 161, 229–242.
- Veizer, J., 1983. Chemical diagenesis of carbonates; theory and application of trace element technique. In: Arthur, M.A., Anderson, T.F., Kaplan, I.R., Veizer, J., Land, L.S. (Eds.), *Stable isotopes in sedimentary geology*, 10. Society for Sedimentary Geology Short Course, pp. 1–100.
- Veizer, J., 1989. Strontium Isotopes in Seawater through Time. *Annual Review of Earth and Planetary Sciences* 17, 141–167.
- Veizer, J., Compston, W., 1974. $^{87}\text{Sr}/^{86}\text{Sr}$ composition of seawater during the Phanerozoic. *Geochim. Cosmochim. Acta* 56, 431–443.
- Veizer, J., Ala, D., Azmy, K., Bruckschen, P., Buhl, D., Bruhn, F., Carden, G.A.F., Diener, A., Ebneth, S., Godderis, Y., 1999. $^{87}\text{Sr}/^{86}\text{Sr}$, $\delta^{13}\text{C}$ and $\delta^{18}\text{O}$ evolution of Phanerozoic seawater. *Chem. Geol.* 161, 59–88.
- Vinogradov, V., Belenitskaya, G., Bujakaite, M., Kuleshov, V., Minaeva, M., Pokrovskii, B., 2006a. Isotopic signatures of deposition and transformation of Lower Cambrian saliferous rocks in the Irkutsk amphitheater: Communication 2. Strontium isotopic composition. *Lithology Mineral Resources* 41, 165–173.
- Vinogradov, V., Belenitskaya, G., Bujakaite, M., Kuleshov, V., Minaeva, M., Pokrovskii, B., 2006b. Isotopic signatures of deposition and transformation of Lower Cambrian saliferous rocks in the Irkutsk Amphitheater: Communication 3. Carbon and oxygen isotopic compositions in carbonates. *Lithology Mineral Resources* 41, 271–279.
- Walter, M.R., Veevers, J.J., Calver, C.R., Gorjan, P., Hill, A.C., 2000. Dating the 840–544 Ma Neoproterozoic interval by isotopes of strontium, carbon, and sulfur in seawater, and some interpretative models. *Precamb. Res.* 100, 371–433.
- Willman, S., Moczydlowska, M., 2008. Ediacaran acritarch biota from the Giles 1 drillhole, Officer Basin, Australia, and its potential for biostratigraphic correlation. *Precamb. Res.* 162, 498–530.
- Yang, J., Sun, W., Wang, Z., Xue, Y., Tao, X., 1999. Variations in Sr and C isotopes and Ce anomalies in successions from China: Evidence for the oxygenation of Neoproterozoic seawater? *Precamb. Res.* 93, 215–233.
- Zachos, J., Pagani, M., Sloan, L., Thomas, E., Billups, K., 2001. Trends, Rhythms, and Aberrations in Global Climate 65 Ma to Present. *Science* 292, 686–693.
- Zhu, M., Zhang, J., Yang, A., 2007. Integrated Ediacaran (Sinian) Chronostratigraphy of South China. *Palaeogeogr. Palaeoclimatol. Palaeoecol.* 254, 7–61.